

The public reporting burden for this collection of information is estimated to average 1 hour per response, including the time for reviewing instructions, searching existing data sources, gathering and maintaining the data needed, and completing and reviewing the collection of information. Send comments regarding this burden estimate or any other aspect of this collection of information, including suggestions for reducing this burden, to Washington Headquarters Services, Directorate for Information Operations and Reports, 1215 Jefferson Davis Highway, Suite 1204, Arlington VA, 22202-4302. Respondents should be aware that notwithstanding any other provision of law, no person shall be subject to any penalty for failing to comply with a collection of information if it does not display a currently valid OMB control number.
PLEASE DO NOT RETURN YOUR FORM TO THE ABOVE ADDRESS.

1. REPORT DATE (DD-MM-YYYY) 22-03-2021	2. REPORT TYPE Final Report	3. DATES COVERED (From - To) 1-Apr-2017 - 30-Nov-2020
---	--------------------------------	--

4. TITLE AND SUBTITLE Final Report: Strengthening and Armoring of Sheared Granular Beds	5a. CONTRACT NUMBER W911NF-17-1-0164
	5b. GRANT NUMBER
	5c. PROGRAM ELEMENT NUMBER 611102

6. AUTHORS	5d. PROJECT NUMBER
	5e. TASK NUMBER
	5f. WORK UNIT NUMBER

7. PERFORMING ORGANIZATION NAMES AND ADDRESSES Yale University Office of Sponsored Projects 25 Science Park - 3rd Floor New Haven, CT 06520 -8327	8. PERFORMING ORGANIZATION REPORT NUMBER
---	--

9. SPONSORING/MONITORING AGENCY NAME(S) AND ADDRESS (ES) U.S. Army Research Office P.O. Box 12211 Research Triangle Park, NC 27709-2211	10. SPONSOR/MONITOR'S ACRONYM(S) ARO
	11. SPONSOR/MONITOR'S REPORT NUMBER(S) 69850-EV.7

12. DISTRIBUTION AVAILABILITY STATEMENT Approved for public release; distribution is unlimited.
--

13. SUPPLEMENTARY NOTES The views, opinions and/or findings contained in this report are those of the author(s) and should not be construed as an official Department of the Army position, policy or decision, unless so designated by other documentation.

14. ABSTRACT

15. SUBJECT TERMS

16. SECURITY CLASSIFICATION OF:			17. LIMITATION OF ABSTRACT	15. NUMBER OF PAGES	19a. NAME OF RESPONSIBLE PERSON Corey O'Hern
a. REPORT UU	b. ABSTRACT UU	c. THIS PAGE UU	UU		19b. TELEPHONE NUMBER +12-034-3242

RPPR Final Report

as of 21-Oct-2021

Agency Code: 21XD

Proposal Number: 69850EV

Agreement Number: W911NF-17-1-0164

INVESTIGATOR(S):

Name: Corey O'Hern
Email: corey.ohern@yale.edu
Phone Number: +12034324258
Principal: Y

Organization: **Yale University**

Address: Office of Sponsored Projects, New Haven, CT 065208327

Country: USA

DUNS Number: 043207562

EIN: 060646973

Report Date: 28-Feb-2021

Date Received: 22-Mar-2021

Final Report for Period Beginning 01-Apr-2017 and Ending 30-Nov-2020

Title: Strengthening and Armoring of Sheared Granular Beds

Begin Performance Period: 01-Apr-2017

End Performance Period: 30-Nov-2020

Report Term: 0-Other

Submitted By: Corey O'Hern

Email: corey.ohern@yale.edu

Phone: (+12) 034-324258

Distribution Statement: 1-Approved for public release; distribution is unlimited.

STEM Degrees: 1

STEM Participants: 4

Major Goals: • Develop a physical understanding of shear-driven granular beds that will enable us to control the resilience of granular beds to erosion from overlying fluid flows.

- Understand the interplay between geometric strengthening and segregation (or armoring), including their relative strength in different parameter regimes.
- Leverage this understanding to design protocols to precisely predict and control the strength of granular beds

The transport of grains by an overlying fluid flow is a fundamental physical process with broad applications in geomorphology, climate science, agriculture, and many other fields. Thus, the ability to predict and control the erosion of granular beds can be used to promote or mitigate erosion, often with significant economic and humanitarian impacts. In the case of hydraulic intake facilities, erosion may be favorable by allowing the removal of collected sediments. On the other hand, the prevention of erosion is crucial in places where bodies of water, land masses, and human development meet.

The yield stress of a granular bed tends to increase with time during fluid flow, meaning that beds tend to become stronger as they are sheared. This fact is well known, but the physical mechanisms behind it are still poorly understood. Our primary goal for this work is to develop a grain-scale understanding for how granular beds become stronger with time to better control their yield strength. We have identified two key mechanisms for bed strengthening. First, granular beds can geometrically strengthen, where the grain-grain forces and contact networks evolve in a way that makes the bed more resistant to shear stress, even in the absence of grain segregation. Second, beds can strengthen through armoring or size segregation, where larger, harder-to-move grains remain at the top of the bed, while smaller grains are either dislodged and flow downstream or fall through holes between large particles into the subsurface. We use complimentary experimental and computational studies to understand these effects in different parameter regimes, including the physical origins of each effect and which effect is dominant under various conditions, such as the flow velocity, grain polydispersity, and turbulent fluctuations. We will then leverage this understanding to design protocols that can precisely control the strength of granular beds.

Accomplishments: The simulation studies have focused on understanding the ensemble-averaged shear modulus in terms of two contributions: one from geometrical families, which are continuously deformed particle packings with the same contact networks, and one from changes in the shear modulus arising from changes in the contact network. Calculations of the shear modulus were performed for packings of spherical particles interacting via several purely repulsive interparticle force laws, including repulsive linear and Hertzian spring interactions.

The experimental studies have focused on understanding the effects of grain size polydispersity on the erodibility and strength of fluid-driven granular beds. Our results indicate that in a polydisperse bed, the small grains control the bed strength, as they are mobilized more easily and their removal destabilizes larger grains. This

RPPR Final Report

as of 21-Oct-2021

result suggests that the common assumption that a polydisperse erodible bed can be described by the mean grain size is likely to be incorrect, and highlights the key (and underappreciated) roles played by the granular contact and force networks.

Computational Studies

During this reporting period, we completed the work on the numerical investigation of the mechanical response of overcompressed frictionless, spherical grains that interact via purely repulsive force laws, which mimic packed granular beds. The particle-particle interactions are governed by the potential, $U(r_{ij}) = \epsilon/\alpha \left[(1 - r_{ij}/\sigma_{ij}) \right]^\alpha \Theta(1 - r_{ij}/\sigma_{ij})$, where r_{ij} is the separation between particle i and j , σ_{ij} is their average diameter, $\Theta(\cdot)$ is the Heaviside step function that prevents particles from interacting if they are not in contact, ϵ is the characteristic energy scale, and α is the power-law scaling exponent of the interaction energy with the amount of particle overlap.

We focus on the ensemble-averaged shear modulus $\langle G \rangle$, which has two main contributions: one from geometrical families, which are jammed packings that have continuous variations in the particle positions, but share the same contact network and one from changes in the shear modulus arising from changes in the contact network (i.e. contact changes and particle rearrangements). It is well-known that the ensemble averaged shear modulus scales as $\langle G \rangle \sim Pa$ at low pressures when $P < P_c$ and as $\langle G \rangle \sim Pb$ when $P > P_c$, where $a \approx (\alpha - 2)/(\alpha - 1)$, $b \approx (\alpha - 3/2)/(\alpha - 1)$, and P_c is the crossover pressure that separates the two scaling regimes. The origin of these exponents remains an open question. In recent work, we have decomposed the isostatic geometrical family contribution to the shear modulus in terms of the affine and nonaffine contributions: $G^a(1) = G_a^a(1) - G_n^a(1)$, where the superscript (1) indicates the first isostatic geometrical family. We showed that the affine contribution to the shear modulus, $G_a^a(1) = (\partial^2 U / \partial \gamma)^2$, where U is the total potential energy of the system, has the following form, $G_a^a(1)/G_0 = \left[(P/P_0) \right]^\alpha ((\alpha - 2)/(\alpha - 1)) - P/P_0$ for $\alpha \geq 2$, as shown in Fig. 1. In this expression, P_0 is the pressure at which $G_a^a(1) = 0$. When $G^a(1) < 0$, the non-affine contribution becomes significant, and $G^a(1)$ begins to deviate from the affine form. (See the insets to Fig. 1 (a) and (b).)

In the current reporting period, we investigated changes in the shear modulus that arise from point (Fig. 2) and jump changes (Fig. 3) in the interparticle contact network. For point changes, the contact network gains or loses a single interparticle contact with negligible particle motion. In addition, point changes are reversible, i.e. if the deformation process is reversed, the system will return to the same particle positions and contacts that existed before the system was deformed. Point changes give rise to discontinuous jumps in G for purely repulsive linear spring interactions (Fig. 2(a)), whereas $G(P)$ is continuous across point changes for Hertzian contacts (Fig. 2(b)). Jump changes in the contact network correspond to mechanical instabilities, involve multiple changes in the contact network, and are irreversible. The shear modulus $G(P)$ is discontinuous across jump changes for both purely repulsive linear and Hertzian spring interactions (Fig. 3).

We also investigated whether the form of the shear modulus for geometrical families depends on which family is considered. In Fig. 4, we show the shear modulus for the second geometrical family. We find that the affine form generally describes the shear modulus for the second geometrical family for purely repulsive linear spring systems, when the first geometrical family ends in a point change or a jump change (Fig. 4 (a)). In contrast, the affine form does not describe the shear modulus near the onset of the second geometrical family for systems with Hertzian spring interactions when a point change causes the end of the first geometrical family (Fig. 4 (b)). For Hertzian spring interactions, the affine form describes the behavior of the shear modulus for the second geometrical family near onset when a jump change causes the end of the first geometrical family (Fig. 4 (c)). For both point and jump changes and for purely repulsive linear and Hertzian spring interactions, the shear modulus for the second geometrical family deviates from the affine form when $G^a(2) < 0$, since the nonaffine contribution increases with pressure. (See insets to Fig. 4.)

We also investigated the contribution of particle rearrangements to the ensemble-averaged shear modulus. The ensemble-averaged shear modulus obeys $\langle G \rangle = \langle G_f \rangle + \langle G_r \rangle$, where $\langle G_f \rangle$ is the contribution from geometrical families and $\langle G_r \rangle$ includes discontinuities in the shear modulus from particle rearrangements and changes in the contact network. In Fig. 5, we show that the rearrangement contribution is comparable to the geometrical family contribution for packings of spherical particles with Hertzian spring interactions, in agreement with our prior results for packings with repulsive linear spring interactions.

We also investigated the system-size dependence of the ensemble-averaged shear modulus $\langle G \rangle$, as shown in Fig. 6. We find that the power-law exponents for $\langle G \rangle$ versus P in the low pressure regime are those expected for the affine form. In the high-pressure regime, we observed deviations from the scaling exponent $b = (\alpha - 3/2)/(\alpha - 1)$,

RPPR Final Report

as of 21-Oct-2021

which has been observed previously for jammed sphere packings. The deviations likely arise from including packings with $G < 0$ in the ensemble average. The frequency of packings with $G < 0$ will be carried out in future studies.

Experimental Studies During this reporting period, the experimental studies focused on understanding the effects of grain polydispersity on the onset of erosion. Classically, polydispersity is accounted for in, e.g., a Shields diagram by simply computing all nondimensional parameters using the mean grain size. However, this approach is overly simplistic, and is unlikely to be correct in detail. In particular, it cannot account for the fact that smaller grains will always be easier to mobilize than larger grains, and so even if the mean grain size can capture typical scaling behavior, it cannot account for this systematic effect.

To study the effects of polydispersity, we conducted experiments for the simplest case: a bimodal bed containing grains of two sizes. We used two sizes of glass beads, and considered three cases: a unimodal bed of small grains, a unimodal bed of large grains, and a 50/50 (by volume) mixture of the two. To distinguish the large and small grains, each size was a different color, which we separated using a clustering algorithm. For consistency of the measurements, we also used two colors in the unimodal beds. Note too that although the bimodal bed contained equal volumes of large and small grains, the local mixture fraction was often more heterogeneous.

RPPR Final Report as of 21-Oct-2021

Training Opportunities: During this reporting period, the current award has supported 6th year Yale MEMS Ph.D. student Philip Wang, who is performed the computational studies of the mechanical properties of granular beds, for both frictional particles, bumpy particles, and spherical particles with different repulsive interparticle potentials. Philip graduated with his Ph.D. in in May, 2021. The award has also supported 5th year Stanford Civil & Environmental Engineering Ph.D. student Marios Galanis, who is performing the experimental work.

In addition, during the summer 2020 PI O'Hern and Philip Wang served as mentors for the ARO's High School Apprenticeship Program (HSAP) and Undergraduate Research Apprenticeship Program (URAP), which supported Katherine Morrissey (a rising senior at Valley Regional High School in Deep River, CT), Mahnav Petersen (a rising senior from Choate Rosemary Hall in Wallingford, CT), and Alice Zhang (a rising junior majoring in Electrical Engineering and Computer Science at Yale). Katherine, Mahnav, and Alice spent eight weeks during the summer 2020 performing computational studies of the structural and mechanical properties of granular packings. In addition, PI O'Hern and Philip Wang served as mentors for the ARO's Research and Engineering Apprenticeship Program (REAP), which provides research experiences for high school students in the New Haven area that are underserved and under-represented in STEM. The REAP participants were Siddhartha Juluru, who is a rising senior at Engineering & Science University Magnet School in West Haven, CT, Jonathan Wang, who is a rising senior at Amity Regional High School in Woodbridge, CT, and Hannah Agwunobi, who is from New Haven, CT and a rising senior at Phillips Academy in Andover, MA. O'Hern will also serve as a REAP mentor for five under-represented high school students during the summer 2021.

An important feature of student training is preparation for oral and poster presentations. Each week, co-PIs O'Hern and Ouellette hold sub-group meetings via teleconference on ARO-funded research, during which the funded students give detailed slide presentations and receive feedback on the prior week's work. O'Hern and Ouellette provide guidance on the proposed calculations and experiments for the upcoming week, as well as discuss bigger picture ideas about the direction of the project. On the Yale side, ARO-funded students are encouraged to attend O'Hern group-wide research meetings each Friday at 10-11A, where one member of the O'Hern group presents their work to other group members. Each member of the group gives a presentation at the O'Hern group meeting at least once each semester. In addition, ARO-funded students are encouraged to give SEAS-wide or other presentations at Yale, such as Yale's hosting of the Northeastern Granular Materials Workshop, Visiting Days for prospective SEAS graduate students, and meetings with departmental seminar speakers. ARO-funded students are also encouraged to attend regional and national scientific meetings to give oral and poster presentations. On the Stanford side, ARO-funded students participate in group meetings and activities as part of the Bob & Norma Street Environmental Fluid Mechanics Laboratory.

Additional computational training is provided by Yale's Center for High Performance Computing, which offers tutorials on MPI parallel programming, GPU optimization, and grant writing for national computing facilities. In 2018, PI O'Hern was awarded a DURIP grant, "A Computing Platform for Modeling Fluid-sheared Granular Beds" that provided number of dedicated GPU servers, which is greatly enhancing our abilities to study computationally armoring and segregation in experimentally relevant settings in 3D with more realistic grain shapes and interactions. In addition, the O'Hern research group was recently awarded 153,000 node hours on the NSF's Texas Advanced Computing Center through XSEDE, 7/1/19 – 12/31/20 and cloud computing resources through Amazon Web Services.

RPPR Final Report

as of 21-Oct-2021

Results Dissemination: Results from the project have been disseminated through published articles, as well as presentations at regional, national, and international scientific workshops and conferences.

A. Presentations

Prof. Corey O'Hern (PI):

1. Duke Kunshan Soft Matter Symposium, Kunshan, China (December 17-20, 2020).
2. Webinars of the Simons Collaboration on Cracking the Glass Problem (June 2, 2021).

B. Journal Articles

1. P. Wang, S. Zhang, P. J. Tuckman, D. Wang, N. T. Ouellette, M. D. Shattuck, and C. S. O'Hern, "Shear response of granular packings compressed above jamming onset," *Phys. Rev. E* (2021); 103(2), 022902.
2. F. Xiong, P. Wang, A. H. Clark, T. Bertrand, N. T. Ouellette, M. D. Shattuck, and C. S. O'Hern, "Comparison of shear and compression jammed packings of frictional disks," *Granular Matter* 21 (2019) 109.
3. M. Galanis, P. Wang, M. D. Shattuck, C. S. O'Hern, and N. T. Ouellette, "Onset of grain motion in eroding subaqueous bimodal granular beds," submitted to *Phys. Rev. Fluids* (2021).

Honors and Awards: Nothing to Report

Protocol Activity Status:

Technology Transfer: Nothing to Report

PARTICIPANTS:

Participant Type: PD/PI

Participant: Corey OHern

Person Months Worked: 1.00

Project Contribution:

National Academy Member: N

Funding Support:

Participant Type: Co PD/PI

Participant: Nicholas Ouellette

Person Months Worked: 1.00

Project Contribution:

National Academy Member: N

Funding Support:

Participant Type: Graduate Student (research assistant)

Participant: Philip Wang

Person Months Worked: 12.00

Project Contribution:

National Academy Member: N

Funding Support:

Participant Type: Graduate Student (research assistant)

Participant: Marios Galanis

Person Months Worked: 12.00

Project Contribution:

National Academy Member: N

Funding Support:

RPPR Final Report

as of 21-Oct-2021

ARTICLES:

Publication Type: Journal Article Peer Reviewed: Y **Publication Status:** 1-Published

Journal: Phys. Rev. Fluids

Publication Identifier Type: DOI

Publication Identifier: 10.1103/PhysRevFluids.2.034305

Volume: 2

Issue:

First Page #: 034305

Date Submitted: 8/25/17 12:00AM

Date Published: 3/31/17 4:00AM

Publication Location:

Article Title: The role of grain dynamics in determining the onset of sediment transport

Authors: A. H. Clark, N. T. Ouellette, M. D. Shattuck, and C. S. O'Hern

Keywords: sediment transport

Abstract: Sediment transport occurs when the nondimensional fluid shear stress τ at the bed surface exceeds a minimum value. A large collection of data, known as the Shields curve, shows that τ_c is primarily a function of the shear Reynolds number Re_τ . It is commonly assumed that $\tau_c > \tau_{c,c}(Re_\tau)$ occurs when the Re_τ -dependent fluid forces are too large to maintain static equilibrium for a typical surface grain. A complementary approach, which remains relatively unexplored, is to identify $\tau_c(Re_\tau)$ as the applied shear stress at which grains cannot stop moving. With respect to grain dynamics, Re_τ can be viewed as the viscous time scale for a grain to equilibrate to the fluid flow divided by the typical time for the fluid force to accelerate a grain over the characteristic bed roughness. We performed simulations of granular beds sheared by a model fluid, varying only these two time scales.

Distribution Statement: 3-Distribution authorized to U.S. Government Agencies and their contractors

Acknowledged Federal Support: Y

Publication Type: Journal Article Peer Reviewed: Y **Publication Status:** 1-Published

Journal: Phys. Rev. Fluids

Publication Identifier Type: DOI

Publication Identifier: <https://doi.org/10.1103/PhysRevFluids.2.114>

Volume: 2

Issue:

First Page #: 114302

Date Submitted: 9/20/18 12:00AM

Date Published: 11/20/17 5:00AM

Publication Location:

Article Title: Determining the onset of hydrodynamic erosion in turbulent flow

Authors: J. C. Salevan, A. H. Clark, M. D. Shattuck, C. S. O'Hern, and N. T. Ouellette

Keywords: hydrodynamic erosion

Abstract: We revisit the longstanding question of the onset of sediment transport driven by a turbulent fluid flow via laboratory measurements. We use particle tracking velocimetry to quantify the fluid flow as well as the motion of individual grains. As we increase the flow speed above the transition to sediment transport, we observe that an increasing fraction of grains are transported downstream, although the average downstream velocity of the transported grains remains roughly constant. However, we find that the fraction of mobilized grains does not vanish sharply at a critical flow rate. Additionally, the distribution of the fluctuating velocities of non-transported grains becomes broader with heavier tails, meaning that unambiguously separating mobile and static grains is not possible. As an alternative approach, we quantify the statistics of grain velocities by using a mixture model consisting of two forms for the grain velocities.

Distribution Statement: 3-Distribution authorized to U.S. Government Agencies and their contractors

Acknowledged Federal Support: Y

RPPR Final Report

as of 21-Oct-2021

Publication Type: Journal Article Peer Reviewed: Y **Publication Status:** 1-Published
Journal: Phys. Rev. E
Publication Identifier Type: DOI Publication Identifier: <https://doi.org/10.1103/PhysRevE.97.062901>
Volume: 97 Issue: First Page #: 062901
Date Submitted: 9/20/18 12:00AM Date Published: 6/6/18 4:00AM
Publication Location:
Article Title: Critical scaling near the yielding transition in granular media
Authors: A. H. Clark, M. D. Shattuck, N. T. Ouellette, and C. S. O'Hern
Keywords: critical scaling, yielding
Abstract: We show that the yielding transition in granular media displays second-order critical-point scaling behavior. We carry out discrete element simulations in the overdamped limit for frictionless, purely repulsive spherical grains undergoing simple shear at fixed applied shear stress τ in two and three spatial dimensions. Upon application of the shear stress, the systems, which were originally isotropically prepared, search for a mechanically stable (MS) packing that can support the applied τ . We measure the strain before each system finds such an MS packing and stops. We show that the density of MS packings obeys critical scaling with a length scale that diverges.
Distribution Statement: 3-Distribution authorized to U.S. Government Agencies and their contractors
Acknowledged Federal Support: Y

Publication Type: Journal Article Peer Reviewed: Y **Publication Status:** 1-Published
Journal: Granular Matter
Publication Identifier Type: DOI Publication Identifier: 10.1007/s10035-019-0964-9
Volume: 21 Issue: 4 First Page #: 109
Date Submitted: 11/2/20 12:00AM Date Published: 11/1/19 8:00AM
Publication Location:
Article Title: Comparison of shear and compression jammed packings of frictional disks
Authors: Fansheng Xiong, Philip Wang, Abram H. Clark, Thibault Bertrand, Nicholas T. Ouellette, Mark D. Shattuck
Keywords: jamming, frictional particles, granular packings
Abstract: We compare the structural and mechanical properties of mechanically stable (MS) packings of frictional disks in two spatial dimensions (2D) generated with isotropic compression and simple shear protocols from discrete element modeling (DEM) simulations. We find that the average contact number and packing fraction at jamming onset are similar (with relative deviations $< 0.5\%$) for MS packings generated via compression and shear. In contrast, the average stress anisotropy $\langle \hat{\Sigma}_{xy} \rangle = 0$ for MS packings generated via isotropic compression, whereas $\langle \hat{\Sigma}_{xy} \rangle > 0$ for MS packings generated via simple shear. To investigate the difference in the stress state of MS packings, we develop packing-generation protocols to first unjam the MS packings, remove the frictional contacts, and then rejam them. Using these protocols, we are able to obtain rejammed packings with nearly identical particle positions and stress anisotropy distributions.
Distribution Statement: 2-Distribution Limited to U.S. Government agencies only; report contains proprietary info
Acknowledged Federal Support: Y

RPPR Final Report

as of 21-Oct-2021

Publication Type: Journal Article Peer Reviewed: Y **Publication Status:** 1-Published
Journal: Phys. Rev. E
Publication Identifier Type: DOI **Publication Identifier:** <https://doi.org/10.1103/PhysRevE.103.02290>
Volume: 103 **Issue:** **First Page #:** 022902
Date Submitted: 3/22/21 12:00AM **Date Published:** 2/17/21 5:00AM
Publication Location:
Article Title: Shear response of granular packings compressed above jamming onset
Authors: P. Wang, S. Zhang, P. J. Tuckman, D. Wang, N. T. Ouellette, M. D. Shattuck, and C. S. O'Hern
Keywords: jamming, mechanical properties, granular materials
Abstract: We investigate the mechanical response of jammed packings of repulsive, frictionless spherical particles undergoing isotropic compression. Prior simulations of the soft-particle model, where the repulsive interactions scale as a power-law in the interparticle overlap with exponent ν , have found that the ensemble-averaged shear modulus G increases with pressure P as $P^{(\nu+3/2)/(\nu+1)}$ at large pressures. However, a deep theoretical understanding of this scaling behavior is lacking. We show that the shear modulus of jammed packings of frictionless, spherical particles has two key contributions: 1) continuous variations as a function of pressure along geometrical families, for which the interparticle contact network does not change, and 2) discontinuous jumps during compression that arise from changes in the contact network.
Distribution Statement: 1-Approved for public release; distribution is unlimited.
Acknowledged Federal Support: Y

Publication Type: Journal Article Peer Reviewed: Y **Publication Status:** 4-Under Review
Journal: Phys. Rev. Fluids
Publication Identifier Type: **Publication Identifier:**
Volume: **Issue:** **First Page #:**
Date Submitted: 3/22/21 12:00AM **Date Published:**
Publication Location:
Article Title: Onset of grain motion in eroding subaqueous bimodal granular beds
Authors: M. Galanis, P. Wang, M. D. Shattuck, C. S. O'Hern, and N. T. Ouellette
Keywords: erosion, granular beds, size polydispersity
Abstract: We report experimental measurements of the onset of grain motion in fully submerged erodible beds containing grains of two sizes driven by a turbulent shear flow. Although we find that a traditional Shields-number framework successfully accounts for grain-size effects in beds composed of grains of only a single size, our results show that bimodal beds are distinct in a way that cannot be captured by a Shields number rescaling. Instead, we find that the hydrodynamic shear stress alone is sufficient to capture the onset of grain motion for both large and small grains, and that the dynamics of the small grains control the onset of motion for the entire bed. By analyzing higher-order statistics, we reveal the key role played by the granular contact and force networks in the bed near onset, and clarify the impact of grain size polydispersity on the transition from a static to an eroding bed. Our results have implications for modeling sediment transport in natural systems.
Distribution Statement: 2-Distribution Limited to U.S. Government agencies only; report contains proprietary info
Acknowledged Federal Support: Y

RPPR Final Report
as of 21-Oct-2021

Partners

,

I certify that the information in the report is complete and accurate:

Signature:

Signature Date:

1. *Major Goals

- Develop a physical understanding of shear-driven granular beds that will enable us to control the resilience of granular beds to erosion from overlying fluid flows.
- Understand the interplay between geometric strengthening and segregation (or armoring), including their relative strength in different parameter regimes.
- Leverage this understanding to design protocols to precisely predict and control the strength of granular beds

The transport of grains by an overlying fluid flow is a fundamental physical process with broad applications in geomorphology, climate science, agriculture, and many other fields. Thus, the ability to predict and control the erosion of granular beds can be used to promote or mitigate erosion, often with significant economic and humanitarian impacts. In the case of hydraulic intake facilities, erosion may be favorable by allowing the removal of collected sediments. On the other hand, the prevention of erosion is crucial in places where bodies of water, land masses, and human development meet.

The yield stress of a granular bed tends to increase with time during fluid flow, meaning that beds tend to become stronger as they are sheared. This fact is well known, but the physical mechanisms behind it are still poorly understood. Our primary goal for this work is to develop a grain-scale understanding for how granular beds become stronger with time to better control their yield strength. We have identified two key mechanisms for bed strengthening. First, granular beds can geometrically strengthen, where the grain-grain forces and contact networks evolve in a way that makes the bed more resistant to shear stress, even in the absence of grain segregation. Second, beds can strengthen through armoring or size segregation, where larger, harder-to-move grains remain at the top of the bed, while smaller grains are either dislodged and flow downstream or fall through holes between large particles into the subsurface. We use complimentary experimental and computational studies to understand these effects in different parameter regimes, including the physical origins of each effect and which effect is dominant under various conditions, such as the flow velocity, grain polydispersity, and turbulent fluctuations. We will then leverage this understanding to design protocols that can precisely control the strength of granular beds.

2. *Accomplished under goals

- The simulation studies have focused on understanding the ensemble-averaged shear modulus in terms of two contributions: one from geometrical families, which are continuously deformed particle packings with the same contact networks, and one from changes in the shear modulus arising from changes in the contact network. Calculations of the shear modulus were performed for packings of spherical particles interacting via several purely repulsive interparticle force laws, including repulsive linear and Hertzian spring interactions.
- The experimental studies have focused on understanding the effects of grain size polydispersity on the erodibility and strength of fluid-driven granular beds. Our results indicate that in a polydisperse bed, the small grains control the bed strength, as they are mobilized more easily and their removal destabilizes larger grains. This result suggests that the common assumption that a polydisperse erodible bed can be described by the mean grain size is likely to be incorrect, and highlights the key (and underappreciated) roles played by the granular contact and force networks.

Computational Studies

During this reporting period, we completed the work on the numerical investigation of the mechanical response of overcompressed frictionless, spherical grains that interact via purely repulsive force laws, which mimic packed granular beds. The particle-particle interactions are governed by the potential, $U(r_{ij}) = \frac{\varepsilon}{\alpha} (1 - \frac{r_{ij}}{\sigma_{ij}})^\alpha \Theta(1 - \frac{r_{ij}}{\sigma_{ij}})$, where r_{ij} is the separation between particle i and j , σ_{ij} is their average diameter, $\Theta(\cdot)$ is the Heaviside step function that prevents particles from interacting if they are not in contact, ε is the characteristic energy scale, and α is the power-law scaling exponent of the interaction energy with the amount of particle overlap.

We focus on the ensemble-averaged shear modulus $\langle G \rangle$, which has two main contributions: one from geometrical families, which are jammed packings that have continuous variations in the particle positions, but share the same contact network and one from changes in the shear modulus arising from changes in the contact network (i.e. contact changes and particle rearrangements). It is well-known that the ensemble averaged shear modulus scales as $\langle G \rangle \sim P^a$ at low pressures when $P < P_c$ and as $\langle G \rangle \sim P^b$ when $P > P_c$, where $a \approx (\alpha - 2)/(\alpha - 1)$, $b \approx (\alpha - 3/2)/(\alpha - 1)$, and P_c is the crossover pressure that separates the two scaling regimes. The origin of these exponents remains an open question. In recent work, we have decomposed the isostatic geometrical family contribution to the shear modulus in terms of the affine and nonaffine contributions: $G^{(1)} = G_a^{(1)} - G_n^{(1)}$, where the superscript (1) indicates the first isostatic geometrical family. We showed that the affine contribution to the shear modulus, $G_a^{(1)} = \frac{\partial^2 U}{\partial \gamma^2}$, where U is the total potential energy

of the system, has the following form, $G_a^{(1)}/G_0 = (P/P_0)^{(\alpha-2)/(\alpha-1)} - P/P_0$ for $\alpha \geq 2$, as shown in Fig. 1. In this expression, P_0 is the pressure at which $G_a^{(1)} = 0$. When $G^{(1)} < 0$, the non-affine contribution becomes significant, and $G^{(1)}$ begins to deviate from the affine form. (See the insets to Fig. 1 (a) and (b).)

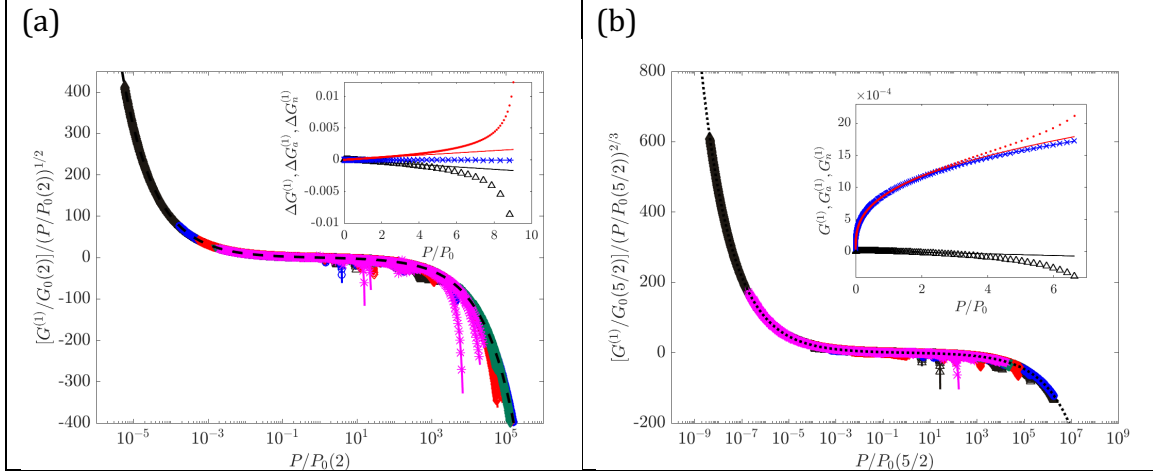


Fig. 1: Shear modulus $G^{(1)}$ versus pressure P for individual isostatic packings with $N=32$ (black upward triangles), 64 (blue circles), 128 (red diamonds), 256 (green downward triangles), and 521 (magenta asterisks) disks within isostatic geometrical families that maintain their interparticle contact networks for purely repulsive (a) linear ($\alpha = 2$) and (b) Hertzian ($\alpha = 5/2$) spring interactions. The dashed line in (a) and dotted line in (b) indicate the affine contribution to $G^{(1)}$, $G_a^{(1)}/G_0 = (P/P_0)^{(\alpha-2)/(\alpha-1)} - P/P_0$, where P_0 is the pressure at which $G_a^{(1)} = 0$. The insets in panels (a) and (b) show $\Delta G^{(1)} = G^{(1)} - G^{(1)}(0)$ (black upward triangles), $\Delta G_a^{(1)} = G_a^{(1)} - G_a^{(1)}(0)$ (blue asterisks), and $\Delta G_n^{(1)} = G_n^{(1)} - G_n^{(1)}(0)$ (red dots), and the solid lines indicate the affine contribution.

In the current reporting period, we investigated changes in the shear modulus that arise from point (Fig. 2) and jump changes (Fig. 3) in the interparticle contact network. For point changes, the contact network gains or loses a single interparticle contact with negligible particle motion. In addition, point changes are reversible, i.e. if the deformation process is reversed, the system will return to the same particle positions and contacts that existed before the system was deformed. Point changes give rise to discontinuous jumps in G for purely repulsive linear spring interactions (Fig. 2(a)), whereas $G(P)$ is continuous across point changes for Hertzian contacts (Fig. 2(b)). Jump changes in the contact network correspond to mechanical instabilities, involve multiple changes in the contact network, and are irreversible. The shear modulus $G(P)$ is discontinuous across jump changes for both purely repulsive linear and Hertzian spring interactions (Fig. 3).

We also investigated whether the form of the shear modulus for geometrical families depends on which family is considered. In Fig. 4, we show the shear modulus for the second geometrical family. We find that the affine form generally

describes the shear modulus for the second geometrical family for purely repulsive linear spring systems, when the first geometrical family ends in a point change or a jump change (Fig. 4 (a)). In contrast, the affine form does not describe the shear modulus near the onset of the second geometrical family for systems with Hertzian spring interactions when a point change causes the end of the first geometrical family (Fig. 4 (b)). For Hertzian spring interactions, the affine form describes the behavior of the shear modulus for the second geometrical family near onset when a jump change causes the end of the first geometrical family (Fig. 4 (c)). For both point and jump changes and for purely repulsive linear and Hertzian spring interactions, the shear modulus for the second geometrical family deviates from the affine form when $G^{(2)} < 0$, since the nonaffine contribution increases with pressure. (See insets to Fig. 4.)

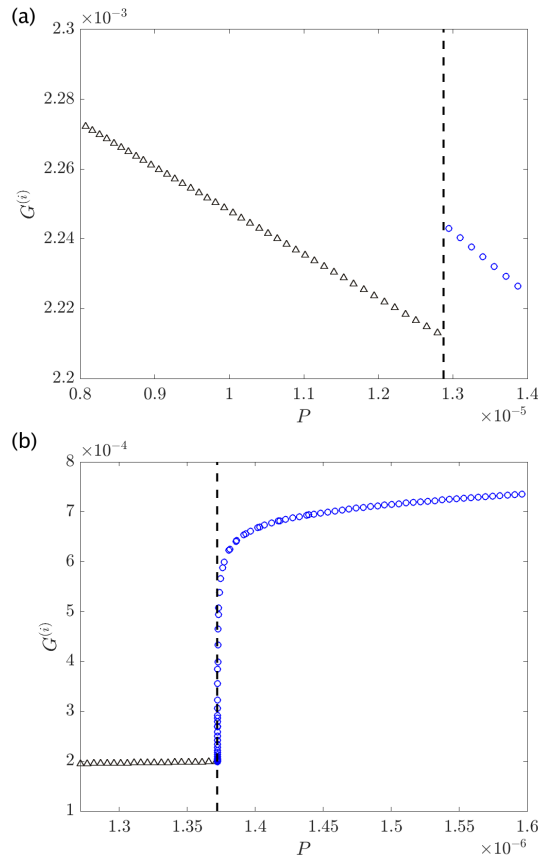


Fig. 2: Point change in the interparticle contact network (indicated by vertical dashed line) during isotropic compression for purely repulsive (a) linear ($\alpha = 2$) and (b) Hertzian ($\alpha = 5/2$) spring interactions. In (a) and (b), the black upper triangles (blue circles) indicate the first (second) geometrical family.

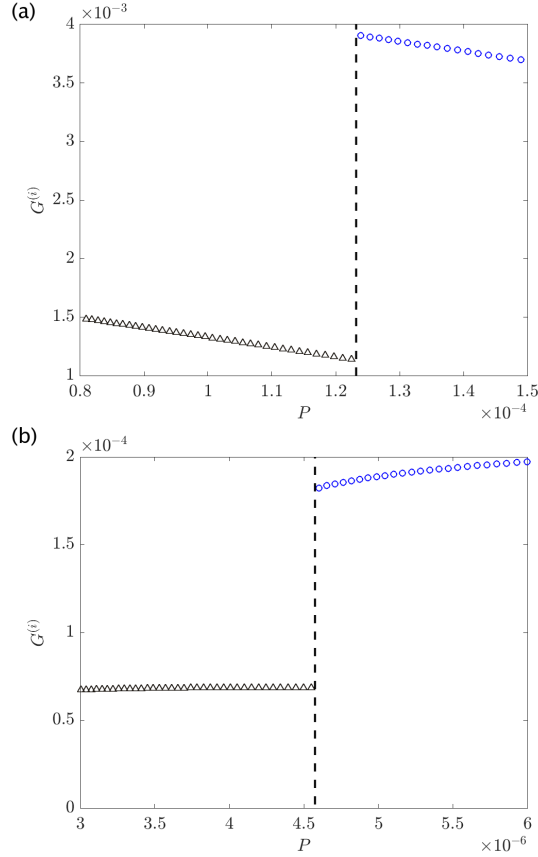


Fig. 3: Jump change in the interparticle contact network (indicated by the vertical dashed line) during isotropic compression for purely repulsive (a) linear ($\alpha = 2$) and (b) Hertzian ($\alpha = 5/2$) spring interactions. In (a) and (b), black upper triangles (blue circles) indicate the first (second) geometrical family.

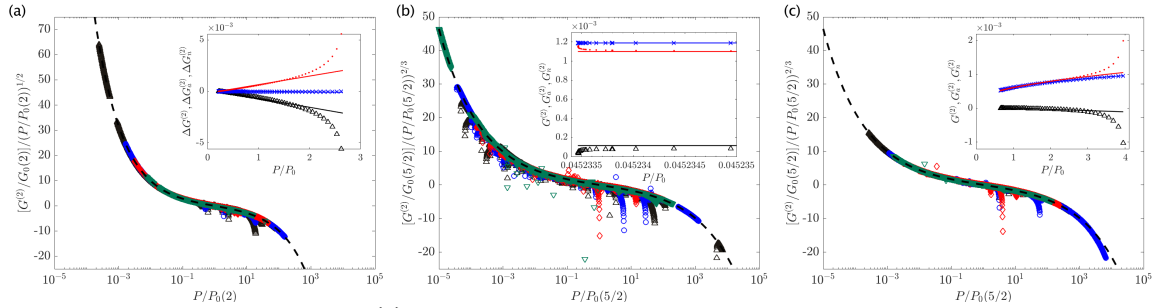


Fig. 4: (a) Shear modulus $G^{(2)}$ versus pressure P for second geometrical family following a point or jump change in the contact network from packings with purely repulsive linear spring interactions. In (b) (and (c)), we show the shear modulus for the second geometrical family with Hertzian interactions following a point change (jump change) that ends the first geometrical family. In (a)-(c), several system sizes are shown: $N=32$ (black upward triangles), 64 (blue circles), 128 (red diamonds) and 256 (green downward triangles). The dashed lines in (a)-(c) indicate the affine contribution to $G^{(2)}$, assuming $G_a^{(2)}/G_0 = (P/P_0)^{(\alpha-2)/(\alpha-1)} - P/P_0$, where P_0 is the pressure at which $G_a^{(2)} = 0$. In the insets to panels (a)-(c), we show $\Delta G^{(2)} = G^{(2)} -$

$G^{(2)}(0)$, $\Delta G_a^{(2)} = G_a^{(2)} - G_a^{(2)}(0)$, and $\Delta G_n^{(2)} = G_n^{(2)} - G_n^{(2)}(0)$, with best fits to the affine form (black, red, and blue solid lines, respectively) for an example $N=32$ packing with purely repulsive linear spring (inset to (a)) and Hertzian interactions (insets to (b) and (c)).

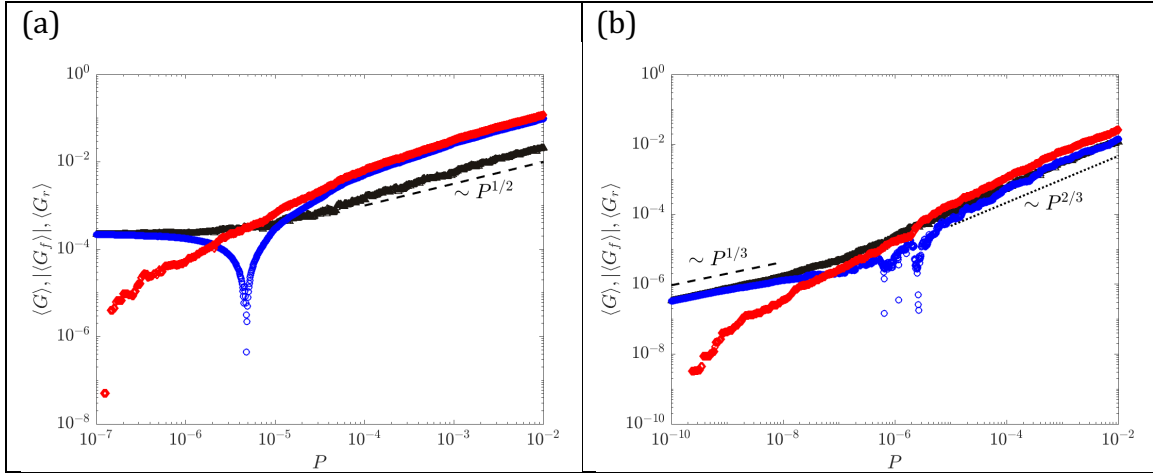


Fig. 5: The ensemble-averaged shear modulus $\langle G \rangle$ (black upward triangles) as a function of pressure for $N = 128$ packings with (a) $\alpha = 2$ and (b) $5/2$ decomposed into contributions from geometrical families $|\langle G_f \rangle|$ (blue circles) and changes in the contact network $\langle G_r \rangle$ (red diamonds). In (a), the dashed line has slope equal to $1/2$ and in (b), the dashed and dotted lines have slopes equal to $1/3$ and $2/3$, respectively.

We also investigated the contribution of particle rearrangements to the ensemble-averaged shear modulus. The ensemble-averaged shear modulus obeys $\langle G \rangle = \langle G_f \rangle + \langle G_r \rangle$, where $\langle G_f \rangle$ is the contribution from geometrical families and $\langle G_r \rangle$ includes discontinuities in the shear modulus from particle rearrangements and changes in the contact network. In Fig. 5, we show that the rearrangement contribution is comparable to the geometrical family contribution for packings of spherical particles with Hertzian spring interactions, in agreement with our prior results for packings with repulsive linear spring interactions.

We also investigated the system-size dependence of the ensemble-averaged shear modulus $\langle G \rangle$, as shown in Fig. 6. We find that the power-law exponents for $\langle G \rangle$ versus P in the low pressure regime are those expected for the affine form. In the high-pressure regime, we observed deviations from the scaling exponent $b = (\alpha - 3/2) / (\alpha - 1)$, which has been observed previously for jammed sphere packings. The deviations likely arise from including packings with $G < 0$ in the ensemble average. The frequency of packings with $G < 0$ will be carried out in future studies.

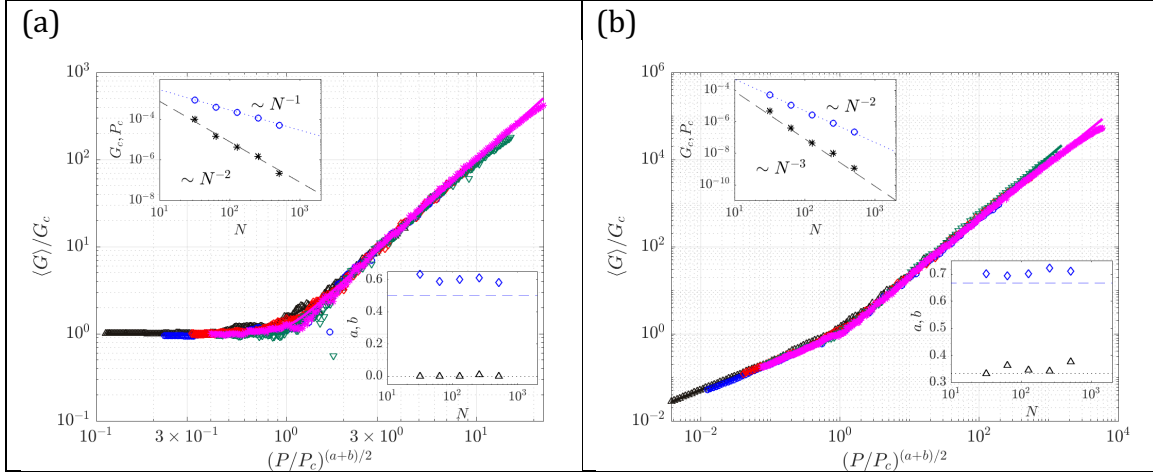


Fig. 6: Ensemble-averaged shear modulus $\langle G \rangle$ versus pressure P for jammed disk packings with repulsive (a) linear and (b) Hertzian spring interactions for system sizes $N=32$ (black upward triangles), 64 (blue circles), 128 (red diamonds), 256 (green downward triangles), and 512 (magenta asterisks). P_c (blue circles in the top left inset in both (a) and (b)) is the characteristic pressure at which $\langle G \rangle$ transitions from one power-law scaling form $\langle G \rangle \sim P^a$ to another $\langle G \rangle \sim P^b$. G_c (black asterisks in the top left inset in both (a) and (b)) is the characteristic shear modulus at which $P = P_c$. The bottom right insets in both (a) and (b) give the power-law exponents a (black upward triangles) and b (blue diamonds) with the dotted and dashed lines located at $a = (\alpha - 2)/(\alpha - 1)$ and $b = (\alpha - 3/2)/(\alpha - 1)$.

Experimental Studies During this reporting period, the experimental studies focused on understanding the effects of grain polydispersity on the onset of erosion. Classically, polydispersity is accounted for in, e.g., a Shields diagram by simply computing all nondimensional parameters using the mean grain size. However, this approach is overly simplistic, and is unlikely to be correct in detail. In particular, it cannot account for the fact that smaller grains will always be easier to mobilize than larger grains, and so even if the mean grain size can capture typical scaling behavior, it cannot account for this systematic effect.

To study the effects of polydispersity, we conducted experiments for the simplest case: a bimodal bed containing grains of two sizes. We used two sizes of glass beads, and considered three cases: a unimodal bed of small grains, a unimodal bed of large grains, and a 50/50 (by volume) mixture of the two. To distinguish the large and small grains, each size was a different color, which we separated using a clustering algorithm. For consistency of the measurements, we also used two colors in the unimodal beds. Note too that although the bimodal bed contained equal volumes of large and small grains, the local mixture fraction was often more heterogeneous.

We then drove fluid shear flows over these beds and analyzed the onset of erosion using the methods we developed in our previous *Physical Review Fluids* paper. As one would expect, we found that the data for the onset of erosion could be collapsed for both unimodal beds when the driving stress was cast in terms of a Shields number using the proper grain size (using the large diameter for the large grains, and small diameter for the small grains). When comparing the data for the large and small grains in the bimodal beds with their unimodal counterparts, however, we found more interesting results. The onset curves for the *small* grains were identical whether those grains were in unimodal or bimodal beds. The onset curves for the *large* grains, however, were different: large grains in the bimodal beds were much more easily mobilized than grains of the same size in a unimodal bed. However, if we plot the data for the *large* grains in the bimodal bed as a function of a Shields number defined for the *small* grains, we observe a much better comparison with the unimodal case. Thus, our data appears to indicate that it is the small grains that control the onset of erosion in the bimodal case, and thus scaling the parameters in the Shields plot by a mean grain size is inappropriate.

We then considered the statistical properties of the bed in more detail by investigating the full probability distributions of the grain velocities near onset. These studies both confirmed our conclusions drawn from our simpler analyses and offered more insight into the detailed mechanisms for the onset of erosion. This work is currently under review at *Physical Review Fluids*.

3. Training Opportunities

During this reporting period, the current award has supported 6th year Yale MEMS Ph.D. student Philip Wang, who is performed the computational studies of the mechanical properties of granular beds, for both frictional particles, bumpy particles, and spherical particles with different repulsive interparticle potentials. Philip graduated with his Ph.D. in in May, 2021. The award has also supported 5th year Stanford Civil & Environmental Engineering Ph.D. student Marios Galanis, who is performing the experimental work.

In addition, during the summer 2020 PI O'Hern and Philip Wang served as mentors for the ARO's High School Apprenticeship Program (HSAP) and Undergraduate Research Apprenticeship Program (URAP), which supported Katherine Morrissey (a rising senior at Valley Regional High School in Deep River, CT), Mahnav Petersen (a rising senior from Choate Rosemary Hall in Wallingford, CT), and Alice Zhang (a rising junior majoring in Electrical Engineering and Computer Science at Yale). Katherine, Mahnav, and Alice spent eight weeks during the summer 2020 performing computational studies of the structural and mechanical properties of granular packings. In addition, PI O'Hern and Philip Wang served as mentors for the ARO's Research and Engineering Apprenticeship Program (REAP), which provides research experiences for high school students in the New Haven area that are underserved and under-represented in STEM. The REAP participants were Siddhartha Juluru, who is a rising senior at Engineering & Science University Magnet

School in West Haven, CT, Jonathan Wang, who is a rising senior at Amity Regional High School in Woodbridge, CT, and Hannah Agwunobi, who is from New Haven, CT and a rising senior at Phillips Academy in Andover, MA. O'Hern will also serve as a REAP mentor for five under-represented high school students during the summer 2021.

An important feature of student training is preparation for oral and poster presentations. Each week, co-PIs O'Hern and Ouellette hold sub-group meetings via teleconference on ARO-funded research, during which the funded students give detailed slide presentations and receive feedback on the prior week's work. O'Hern and Ouellette provide guidance on the proposed calculations and experiments for the upcoming week, as well as discuss bigger picture ideas about the direction of the project. On the Yale side, ARO-funded students are encouraged to attend O'Hern group-wide research meetings each Friday at 10-11A, where one member of the O'Hern group presents their work to other group members. Each member of the group gives a presentation at the O'Hern group meeting at least once each semester. In addition, ARO-funded students are encouraged to give SEAS-wide or other presentations at Yale, such as Yale's hosting of the Northeastern Granular Materials Workshop, Visiting Days for prospective SEAS graduate students, and meetings with departmental seminar speakers. ARO-funded students are also encouraged to attend regional and national scientific meetings to give oral and poster presentations. On the Stanford side, ARO-funded students participate in group meetings and activities as part of the Bob & Norma Street Environmental Fluid Mechanics Laboratory.

Additional computational training is provided by Yale's Center for High Performance Computing, which offers tutorials on MPI parallel programming, GPU optimization, and grant writing for national computing facilities. In 2018, PI O'Hern was awarded a DURIP grant, "A Computing Platform for Modeling Fluid-sheared Granular Beds" that provided number of dedicated GPU servers, which is greatly enhancing our abilities to study computationally armoring and segregation in experimentally relevant settings in 3D with more realistic grain shapes and interactions. In addition, the O'Hern research group was recently awarded 153,000 node hours on the NSF's Texas Advanced Computing Center through XSEDE, 7/1/19 - 12/31/20 and cloud computing resources through Amazon Web Services.

4. Results Dissemination

Results from the project have been disseminated through published articles, as well as presentations at regional, national, and international scientific workshops and conferences.

A. Presentations

Prof. Corey O'Hern (PI):

1. Duke Kunshan Soft Matter Symposium, Kunshan, China (December 17-20, 2020).
2. Webinars of the Simons Collaboration on Cracking the Glass Problem (June 2, 2021).

B. Journal Articles

1. P. Wang, S. Zhang, P. J. Tuckman, D. Wang, N. T. Ouellette, M. D. Shattuck, and C. S. O'Hern, "Shear response of granular packings compressed above jamming onset," *Phys. Rev. E* (2021); 103(2), 022902.
2. F. Xiong, P. Wang, A. H. Clark, T. Bertrand, N. T. Ouellette, M. D. Shattuck, and C. S. O'Hern, "Comparison of shear and compression jammed packings of frictional disks," *Granular Matter* 21 (2019) 109.
3. M. Galanis, P. Wang, M. D. Shattuck, C. S. O'Hern, and N. T. Ouellette, "Onset of grain motion in eroding subaqueous bimodal granular beds," submitted to *Phys. Rev. Fluids* (2021).

5. *Plans for next reporting period

- For the computational studies, we will study the shear modulus, both the contributions from geometrical families and from particle rearrangements, of jammed packings of nonspherical particles, such as circulo-lines.
- In the experimental studies, we will extend our work on the effects of grain size polydispersity to investigate how the local mixture fraction on the surface of the bed drives patchiness in the erosion behavior, following the hypothesis that regions that locally have a higher than average proportion of small grains should erode more easily than those with a higher proportion of large grains. In addition, we will study how cyclic fluid-driving affects the strength of polydisperse granular beds.

Computational Studies In future work, we will carry out studies to understand the scaling of the shear modulus with pressure in packings of circulo-lines in two spatial dimensions (Fig. 7). In preliminary studies, we find that the shear modulus of near-isostatic geometrical families typically increases with pressure for packings of circulo-lines. In contrast, the shear modulus of near-isostatic geometrical families decreases with pressure for disk packings (Fig. 8). We find that the ensemble-averaged shear modulus for packings of circulo-lines scales as $\langle G \rangle \sim P^b$, where $b > 0.5$ in the large pressure limit. In future studies, we will determine the relative contributions of particle rearrangements and geometrical families to $\langle G \rangle$ for packings of nonspherical particles.

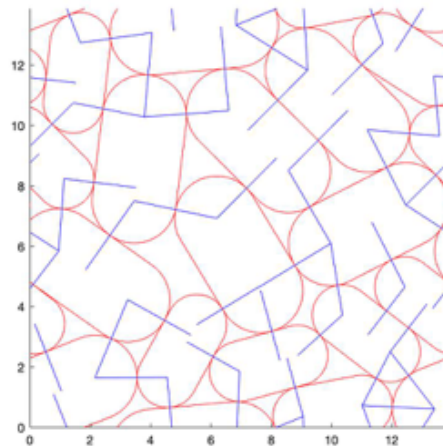


Fig. 7: Snapshot of a jammed packing of $N=16$ circulo-lines with aspect ratio $A=2$. Half of the circulo-lines are large and half are small with diameter ratio $r=1.4$. The blue solid lines correspond to interparticle contacts.

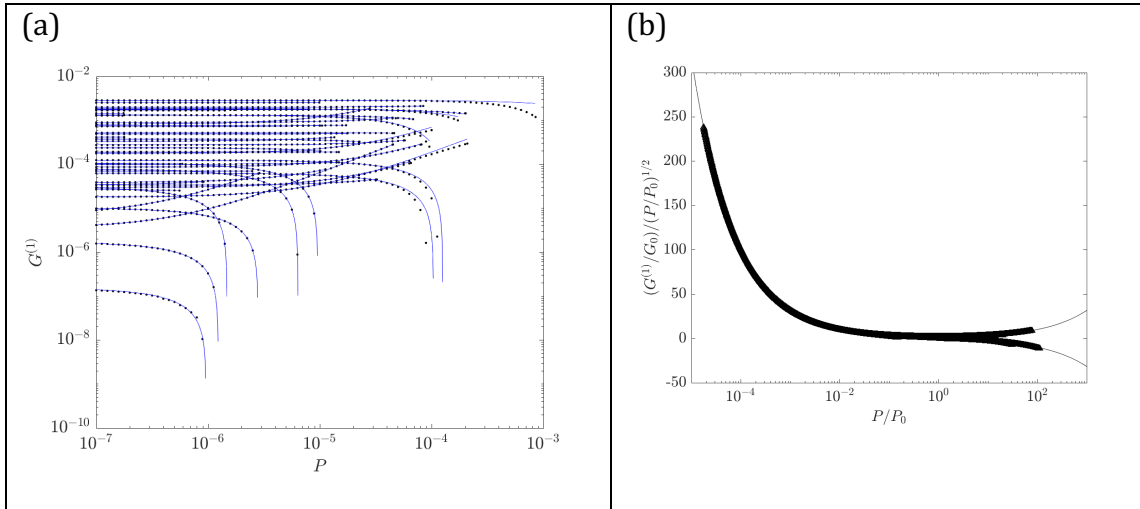


Fig. 8: (a) The shear modulus for isostatic geometrical families $G^{(1)}(P)$ as a function of pressure P for packings of circulo-lines. The solid solids are fits to $G^{(1)}(P) = A \pm BP$, where A and B are constants that depend on the initial conditions. (b) Best fits of the data in (a) to the dimensionless form, $\frac{G^{(1)}}{G_0} \left(\frac{P}{P_0}\right)^{-1/2} = \left(\frac{P}{P_0}\right)^{-1/2} \mp \left(\frac{P}{P_0}\right)^{1/2}$.

Experimental Studies In the future work, we propose to study the effects of stress history and flow reversals on the bed stability, for both monodisperse and polydisperse grain size distributions. We will quantify both how this stress history modifies the onset of grain motion and whether grain polydispersity enhances or weakens these effects. We will also study the spatial distribution of erosion in polydisperse beds with the goal of connecting it to the local grain size distribution.

6. Honors and Awards

N/A